Journal of Physics D: Applied Physics

PAPER

Liquid-crystal-based tunable plasmonic waveguide filters

To cite this article: Shengtao Yin *et al* 2018 *J. Phys. D: Appl. Phys.* **51** 235101

IOP Publishing

Journal of Physics D: Applied Physics

J. Phys. D: Appl. Phys. **51** (2018) 235101 (6pp)

https://doi.org/10.1088/1361-6463/aac0aa

Liquid-crystal-based tunable plasmonic waveguide filters

Shengtao Yin[1,2], Yan Jun Liu[1], Dong Xiao[1], Huilin He[1], Dan Luo[1], Shouzhen Jiang[3], Haitao Dai[4], Wei Ji[2] and Xiao Wei Sun[1]

[1] Department of Electrical and Electronic Engineering, Southern University of Science and Technology, Shenzhen 518055, People's Republic of China
[2] School of Information Science and Engineering, Shandong University, Jinan 250000, People's Republic of China
[3] School of Physics and Electronics, Shandong Normal University, Jinan 250014, People's Republic of China
[4] Tianjin Key Laboratory of Low Dimensional Materials Physics and Preparing Technology, School of Science, Tianjin University, Tianjin 300072, People's Republic of China

E-mail: yjliu@sustc.edu.cn and jiwww@sdu.edu.cn

Received 7 January 2018, revised 15 April 2018
Accepted for publication 27 April 2018
Published 15 May 2018

CrossMark

Abstract

We propose a liquid-crystal-based tunable plasmonic waveguide filter and numerically investigate its filtering properties. The filter consists of a metal-insulator-metal waveguide with a nanocavity resonator. By filling the nanocavity with birefringent liquid crystals (LCs), we could then vary the effective refractive index of the nanocavity by controlling the alignment of the LC molecules, hence making the filter tunable. The tunable filtering properties are further analyzed in details via the temporal coupled mode theory (CMT) and the finite-difference time-domain (FDTD) method. The simulation results show that the resonant wavelengths have linear redshift as the refractive index of the nanocavity increases and the coupling efficiency is more than 65% without considering the internal loss in the nanocavity and waveguides. These achieved results by the FDTD simulations can be also accurately analyzed by CMT. The compact design of our proposed plasmonic filters is especially favorable for integration, and such filters could find many important potential applications in high-density plasmonic integration circuits.

Keywords: liquid crystal, plasmonics, wavelength filtering device, waveguide

(Some figures may appear in colour only in the online journal)

Introduction

Plasmonics is a rapid developing research subfield in photonics dedicated to the fundamental studies and applications of surface plasmons (SPs). SPs are essentially a special kind of light formed by collective free electron oscillations at the interfaces of metals and dielectric materials [1, 2], which can only propagate at the metal/dielectric interface and decay exponentially away from the interface. The strong and unique capability of SPs to manipulate light at the nanoscale has led to numerous intriguing physical phenomena [3–5] and useful applications [6–9]. One of most important research directions on plasmonics is the development of nanophotonic circuits/chips [10], which could take full advantage of unique properties of SPs. Therefore, a number of waveguide-type plasmonic devices have been proposed, developed and integrated to realize specific chip-based optical functions. Along this line, various plasmonic nanostructures have been designed for guiding/processing plasmonic signal efficiently, such as nanoparticle chain waveguides [11], gap-stripe waveguides [12], semi-conductor nanowire [13], photonic bandgap waveguides [14], and so on.

Among them, the metal-insulator-metal (MIM) nanostructures have attracted intensive attention due to the strong confinement of light and excellent compromise between propagation length and losses [15]. Thus far, a variety of functional plasmonic devices based on MIM waveguides haven been theoretically proposed and experimentally realized, such as optical splitters [16], optical switches [17], Mach-Zehnder interferometers [18], sensors [19], absorbers [20], and optical filters [21, 22]. Specifically, plasmonic filters, as a crucial component, play an important role in multi-functional photonic chips by providing wavelength-selection. MIM waveguide-type plasmonic filter can reduce the fabrication complexity and increase the prorogation length for SPPs. Hence, some simple plasmonic waveguide filters have been proposed including ring resonators [23], tooth-shaped plasmonic waveguide filters [24], rectangular geometry resonators [25] and channel drop filters with disk resonators [26]. Most of them have the configuration of MIM waveguides coupled with a gear-shaped cavity [27], a ring cavity [28], a rectangular cavity [29], a nanodisk cavity [30], and so on. However, most of the current plasmonic waveguide filters are passive, which means the filtering function is fixed upon fabrication and lacks efficient control of plasmonic signal. Future development requires the filters to have switchable or tunable capability under external stimuli—so called active control.

Researchers have put tremendous efforts to develop active plasmonic devices. One effective way is to take advantage of the eminent property of SPs—the high sensitivity to the surrounding dielectric materials of the plasmonic nanostructures [31–33]. The use of tunable dielectric materials has proved to be a very efficient approach for active plasmonics [34–38]. For example, Wang and Chumanov have demonstrated the electrochemical modulation of the intensity and frequency of LSPR in Ag nanoparticles embedded in a tungsten oxide matrix [39]. Zheng *et al* have achieved active tuning of the plasmon resonances in rotaxane—coated gold nanodisk arrays by chemically switching the rotaxane molecules between its oxidized and reduced states [40].

Liquid crystals (LCs) stand out from all the rest due to its large birefringence on refractive index, low threshold on transition among different states, fluid nature for easy integration, and versatile driven methods to cause the transitions. These distinctive advantages make it an excellent candidate for active plasmonics [41, 42]. So far, both electrical [43–51] and optical tuning [52–55] of plasmonic properties have been demonstrated based on reorientation of the LC molecules. In this paper, we propose a plasmonic waveguide filter that consists of a circular nanocavity filled with nematic LCs coupled with two MIM waveguides symmetrically. The wavelength-tuning properties of resonant modes in the nanocavity, the transmission characteristics, including the transmission efficiency, resolution and relevant SPP mode distributions are analyzed by employing the finite-difference time-domain (FDTD) method [56]. The transmission characteristics can be explained by the temporal coupled mode theory (CMT) [57]. The obtained results shows that our proposed plasmonic waveguide filters have big potential for high-density, integrated plasmonic chips/circuits. For instance, it can work as an optical switch/modulator to modulate the transmitted optical signal in the integrated plasmonic circuits.

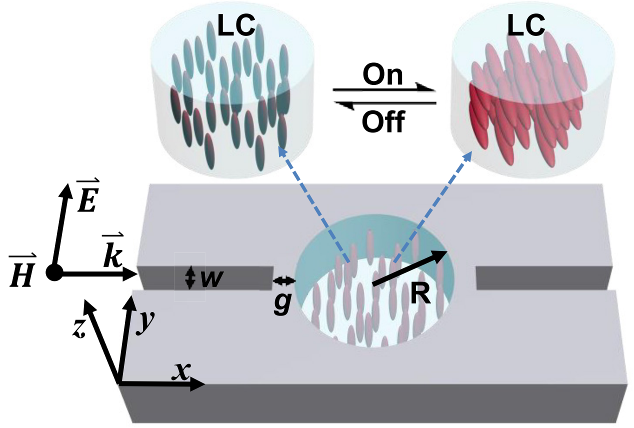

Figure 1. Schematic diagram of the plasmonic waveguide filter structure composed of two slits, two semi-infinite metallic claddings, and a LC-filled nanocavity resonator in the middle of the MIM structure. The important geometrical parameters are defined in this structure.

Structure and theoretical analysis

The structural configuration of the proposed plasmonic waveguide filter is schematically shown in figure 1, which consists of a circular nanocavity filled with NLCs in the middle of a MIM waveguide slit. This structure possesses mirror symmetry. The width of the air slit is w. The coupling distance between the nanocavity and the MIM waveguide is g. The circular nanocavity has the radius of R. The insulator layer and the metal layer of the MIM waveguide are set as air ($\varepsilon_{\mathrm{Air}} = 1.0$) and silver, respectively. The permittivity ε_{m} of the silver can be described by the Drude model [58]:

$$\varepsilon_m(\omega) = \frac{\varepsilon_\infty - \omega_p^2}{\omega_i(\omega_i + i\gamma)}, \tag{1}$$

where ω_{i} is the angular frequency of the incident light, ω_{p} is the bulk plasma frequency, γ is the electron collision frequency. ε_∞ is the dielectric constant at the infinite frequency. The parameters for the silver metal layer can be set as $\omega_{\mathrm{p}} = 9.1\,\mathrm{eV}$, $\gamma = 0.018\,\mathrm{eV}$, $\varepsilon_{\mathrm{m}} = 3.7$.

Based on the temporal CMT [59], the transmission of this structure can be expressed as:

$$T(\omega) = \left|\frac{\tau_i}{j\tau_\omega\tau_i(\omega - \omega_0) + \tau_\omega + \tau_i}\right|^2, \tag{2}$$

where ω is the angular frequency of the input wave, ω_0 is the resonant frequency in cavity, $1/\tau_{\mathrm{i}}$ and $1/\tau_\omega$ are the decay rates due to the intrinsic loss and the waveguide coupling loss, respectively. We can find that the transmission spectra around the resonant modes exhibit Lorentzian profiles. When the incident light is the resonant wavelength exactly, the transmission can be described as:

$$T(\omega_0) = \left|\frac{\tau_i}{\tau_\omega + \tau_i}\right|^2. \tag{3}$$

At the resonant frequency ω_0, the cavity mode is excited and the incident light is transmitted. Far from the resonant

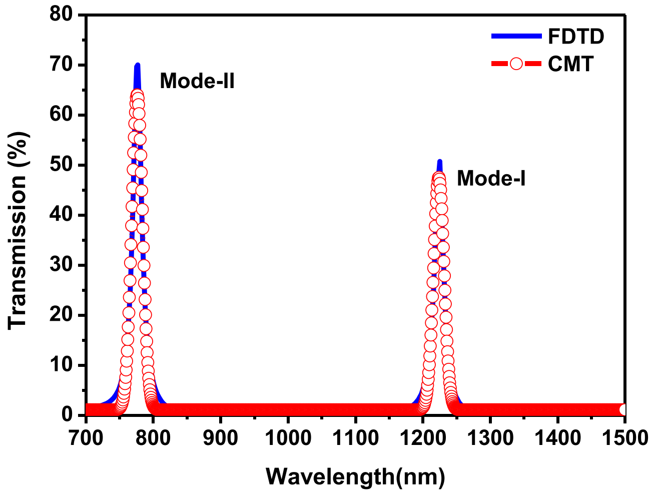

Figure 2. FDTD and CMT simulated transmission spectrum of the plasmonic waveguide filter. The refractive index of the LC-filled nanocavity is 1.52.

frequency, the incident mode is almost completely reflected. When $1/\tau_i$ is far less than $1/\tau_w$, the resonant wavelength transmission peak is close to 100%.

The structure's plasmonic resonant wavelength satisfies the eigenvalue equation which can be given as follows [60, 61]:

$$\begin{vmatrix} J_m\left(\frac{2\pi n_1 R}{\lambda}\right) & H_m^{(1)\prime}\left(\frac{2\pi n_2 R}{\lambda}\right) \\ \frac{J_m'\left(\frac{2\pi n_1 R}{\lambda}\right)}{n_1} & \frac{H_m^{(1)\prime}\left(\frac{2\pi n_2 R}{\lambda}\right)}{n_2} \end{vmatrix} = 0. \quad (4)$$

J_m and J_m' are the first kind Bessel function with the mth order and its derivation function, $H_m^{(1)}$ and $H_m^{(1)\prime}$ are the first kind Hankel function with the mth order and its derivation function, respectively. n_1 and n_2 are the refractive indices of the insulator's waveguides and the NLCs inside the nanocavity, respectively. λ is the resonant wavelength. R is the radius of the nanocavity. From the equation we can summarize that the resonant wavelength λ is determined by the radius of the nanocavity, R and the refractive index of the MIM structure. Thus, we can tune the refractive index of the NLCs to select the specific resonant wavelength.

Simulation results and analysis

In order to understand the theoretical analysis above, both FDTD and CMT simulation are used to calculate the transmission characteristics of the proposed structure. The structural parameters have been numerically optimized through a large number of simulations. In our simulations, the optimal geometrical parameters are chosen as $w = 31$ nm, $g = 20$ nm, $R = 200$ nm. The wavelength range of the light source is set 700 nm to 1500 nm. The refractive index of the LC-filled nanocavity can be estimatedly tuned from 1.52 to 1.74 [62]. The dielectric function of the silver is described by the Drude model. The refractive index of the air is 1.0. In our simulation, the mesh size was set to 3 nm and 2D simulation was carried out for our proposed structures.

Figure 2 shows the simulated results of our proposed plasmonic waveguide filter. The polarization of the incident light source is along y-axis. From the transmission spectrum (figure 2) in our interested wavelength range, we can see clearly that there are two distinct and sharp resonant transmission peaks (marked as Mode-I and Mode-II) that locate at the wavelength of 1225 nm and 777 nm, respectively, which exhibit typical filtering characteristics for both modes. To further investigate the underlying physical origins of the resonant modes, we calculate the magnetic-field and corresponding charge distributions at the peak positions for both Mode-I and Mode-II, as shown in figures 3(a)–(d), respectively. From figure 3, it is obvious that Mode-I shows the dipolar resonance, while Mode-II demonstrates the quadrupolar resonance. It can be seen that the excitations of resonant modes happen inside the nanocavity at the wavelengths of 1225 nm and 777 nm, indicating that the incident light with the resonant wavelengths can pass through the MIM plasmonic structure. In contrast, the incident light out of the resonance is then blocked as there is no excitation of resonant modes.

In general, it is well known that the plasmonic nanocavity is highly sensitive to the surrounding medium. In our design, the circular nanocavity is filled with LCs, whose refractive index can be effectively tuned by controlling the alignment of LC molecules. Therefore, we expect that the resonant modes of the plasmonic nanocavity can be then tuned due to the change of the effective refractive index inside the nanocavity. As a result, our proposed plasmonic waveguide filters will demonstrate a tunable filtering properties. As a proof-of-concept, we employ a widely used LC, E7, in our simulation. The LC E7 is a well-studied anisotropic material. Its wavelength-dependent ordinary and extraordinary refractive indices can be described by the extended Cauchy model. The detailed description can be found in the previous report [62]. The transmission spectra of the structure were simulated as the effective refractive index of the LC-filled nanocavity was tuned from 1.52 to 1.74. The tuning of the refractive index could be realized by controlling the alignment of LC molecules under an external electric field [47, 48]. The simulated results are illustrated in figures 4(a) and (b), respectively. From figure 4(a), we can see that the peak wavelengths of both resonant modes (Mode-I and Mode-II) have a redshift with the increase of the effective refractive index. Figure 4(b) shows the peak positions of both Mode-I and Mode-II as a function of the refractive index of the nanocavity, which demonstrate a nearly linear relationship. The simulation results show that Mode-I and Mode-II have the sensitivity of ~80 and ~50 nm/RIU, respectively. Therefore, one can externally tune the refractive index of the filled LCs inside the nanocavity to achieve the desired filtering wavelength to a specific propagating channel.

The filtering properties of the plasmonic waveguide filter are further investigated by replotting the transmission spectra together with the change of the refractive index, as shown in figure 5(a). It can be clearly observed that the transmittance has a gradual decrease for both Mode-I and Mode-II. In addition, the transmittance of Mode-I is lower than that of Mode-II, indicating that Mode-II has a higher coupling efficiency than that of Mode-I. This might be attributed to the fact that Mode-II has a larger $1/\tau_w$ compared to Mode-I. The coupling efficiency can be analyzed by CMT and calculated

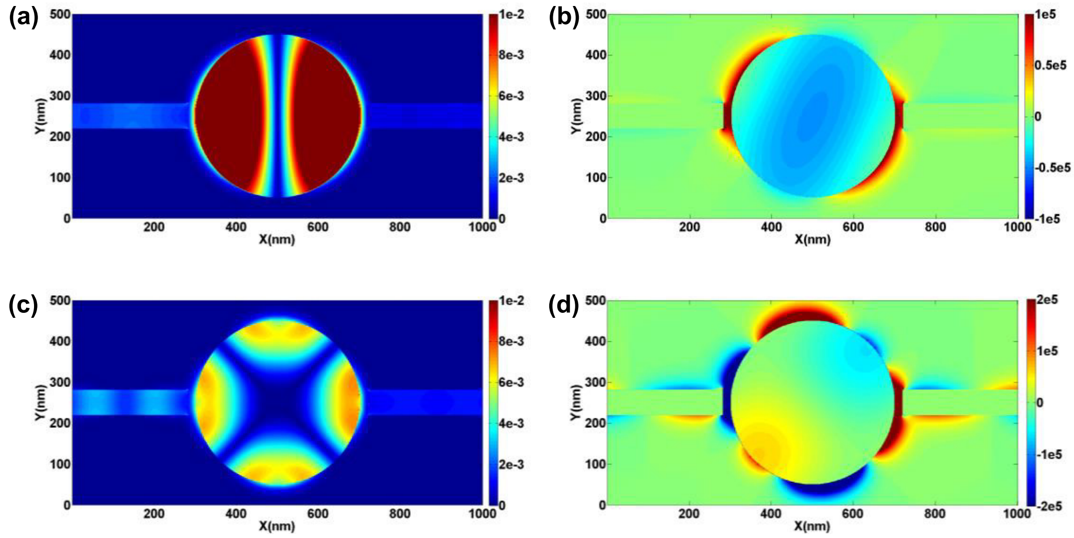

Figure 3. Simulated magnetic-field ((a) and (c)) and corresponding charge ((b) and (d)) distributions at the peak positions of Mode-I ((a) and (b)) and Mode-II ((c) and (d)), respectively.

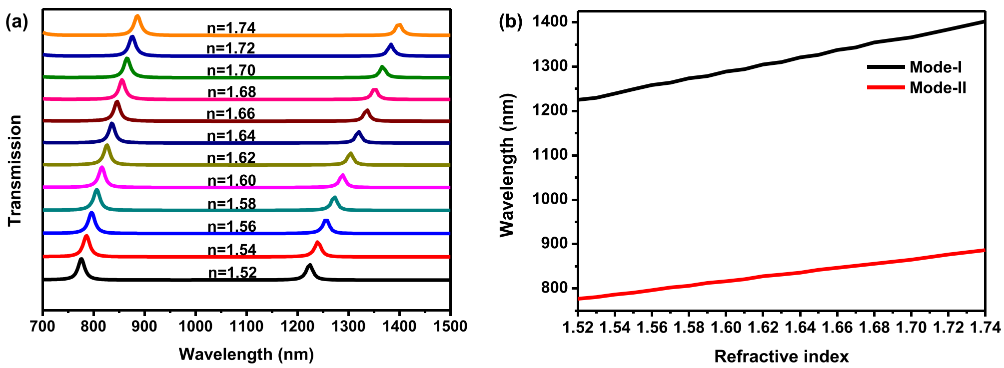

Figure 4. (a) Transmission spectra of the plasmonic waveguide filter with different refractive indices of the LC-filled nanocavity. (b) The evolution of the peak positions of Mode-I and Mode-II as a function of the refractive index of the LC-filled nanocavity.

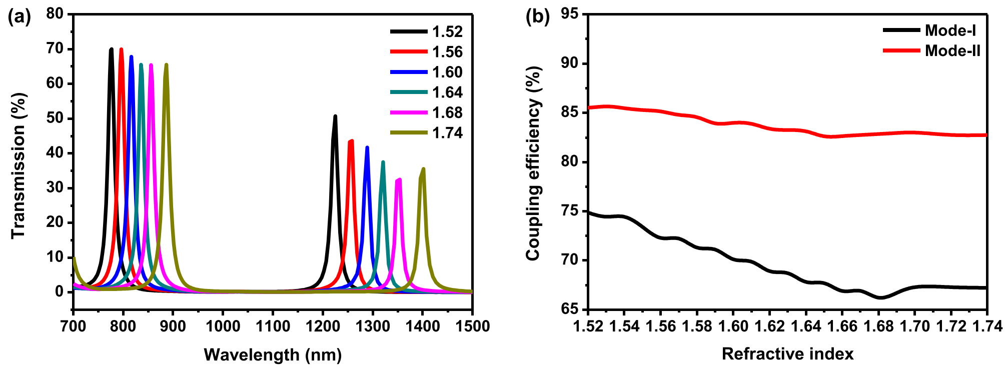

Figure 5. (a) Evolution of transmission spectra of the plasmonic waveguide filter as a function of the refractive index of the LC-filled nanocavity. (b) The calculated coupling efficiencies of Mode-I and Mode-II with different refractive indices of the LC-filled nanocavity.

by FDTD simulation. Figure 5(b) shows the simulation result of the coupling efficiency of Mode-I and Mode-II. We can see that as the refractive index of the LC increases, the coupling efficiency decreases fluctuantly. However, overall in the range of 1.5 to 1.7, the coupling efficiencies of Mode-I and Mode-II are above 65% and 75%, respectively, which are sufficient for filtering purpose.

For the filters, the full-width at half-maximum (FWHM) of the filtering peak is also an important parameter that cannot be ignored during the design process. We find that the filtering bandwidth can be further reduced by cascading multiple circular nanocavities in the plasmonic waveguide. In our design, we further investigate the filtering bandwidth (i.e. FWHM) by taking the Mode-II for example. Figures 6(a) and (b) shows

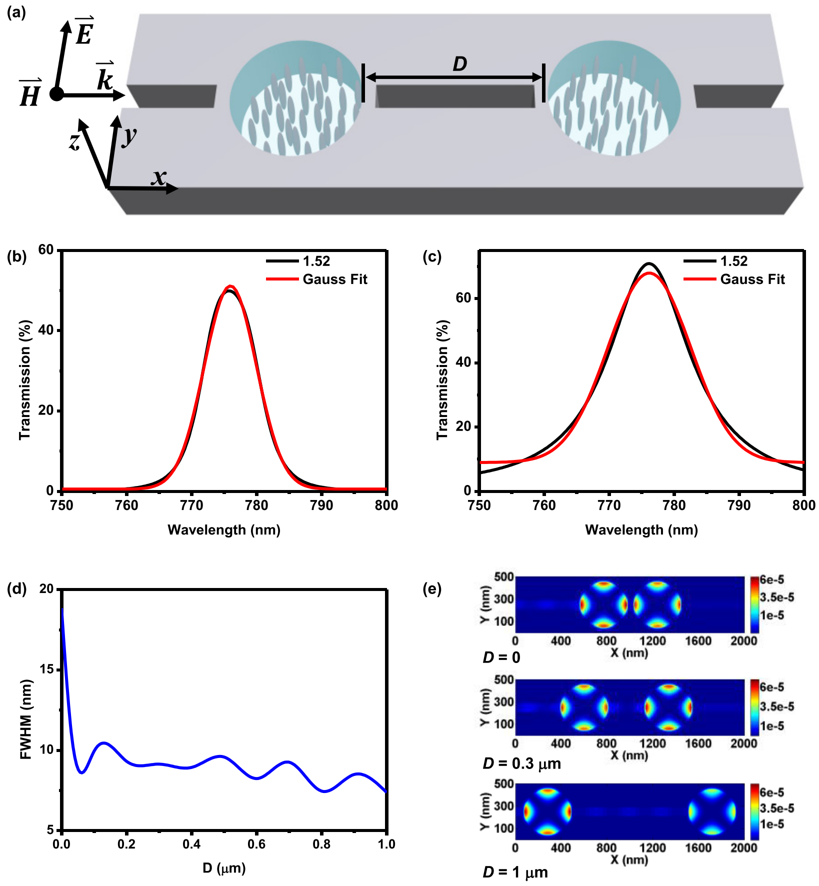

Figure 6. (a) Schematic diagram of the plasmonic waveguide filter structure with two cascaded LC-filled nanocavities. (b) The calculated FWHM of Mode-II for the case with two cascaded LC-filled nanocavities and the effective index of 1.52 of LC-filled nanocavities. (c) The calculated FWHM of Mode-II for the case with only one LC-filled nanocavity. (d) The effect of the gap distance between two nanocavities on the FWHM. (e) Magnetic-field distribution at different gap distances.

the schematic of the plasmonic waveguide filter with two cascaded nanocavities and the corresponding simulation results. From figure 6(b), the calculated filtering bandwidth is about 8 nm by fitting the transmission peak using the Gaussian function. For comparison, figure 6(c) shows the filtering bandwidth with only one circular nanocavity in the MIM plasmonic waveguide. The filtering bandwidth is about 15 nm, which is almost twice increment of the bandwidth compared to the case of two cascaded nanocavities. The reduction of the FWHM is mainly attributed to the coupling effect of the cascaded nanocavities. Figures 6(d) and (e) shows the effect of the gap distance *D* on the FWHM and corresponding magnetic-field distribution at different gap distances. However, it is worth noting that the transmission power for the case of two cascaded nanocavities also decreases because of the intrinsic loss and waveguide coupling loss. As a result, one can design such kind of plasmonic waveguide filters with desired performance by compromising the filtering bandwidth and transmission power.

Conclusion

In summary, we have proposed a LC-based plasmonic waveguide filter with tunable filtering properties. The designed filter consists of a MIM waveguide with a nanocavity resonator. By filling the nanocavity with birefringent LCs, we can then vary the effective refractive index of the nanocavity by controlling the alignment of the LC molecules, hence making the filter tunable. The obtained results are in good agreement between the CMT and FDTD methods. The simulation results show that the resonant wavelengths have linear redshift as the refractive index of the nanocavity increases. Moreover, the filtering bandwidth can be also adjusted by cascading multiple circular nanocavities in the plasmonic waveguide. The design is compact and straightforward, which is favorable for simple and easy fabrication and integration as well. Our proposed plasmonic filters could find many important potential applications in high-density plasmonic integration circuits.

Acknowledgments

We acknowledge the financial support from Natural Science Foundation of Guangdong Province (Grant No. 2017A030313034), Shenzhen Science and Technology Innovation Council (Grant Nos. JCYJ20170817111349280 and KQTD20160301112030005), and the start-up fund provided by Southern University of Science and Technology (SUSTech).

This work is also partially supported by National Natural Science Foundation of China (NSFC) (Grant No. 61571273).

ORCID iDs

Yan Jun Liu https://orcid.org/0000-0001-8724-0434

References

[1] Raether H 1988 *Surface Plasmons on Smooth and Rough Surfaces and on Gratings* (Berlin: Springer)
[2] Maier S A 2007 *Plasmonics: Fundamentals and Applications* (Berlin: Springer)
[3] Ebbesen T W, Lezec H J, Ghaemi H F, Thio T and Wolff P A 1998 *Nature* **86** 1114–7
[4] Pendry J B 2000 *Phys. Rev. Lett.* **85** 3966–9
[5] Yu N, Genevet P, Kats M A, Aieta F, Tetienne J-P, Capasso F and Gaburro Z 2011 *Science* **334** 333–7
[6] Fang N, Lee H, Sun C and Zhang X 2005 *Science* **308** 534–7
[7] Laux E, Genet C, Skauli T and Ebbesen T W 2008 *Nat. Photon.* **2** 161–4
[8] Si G Y *et al* 2013 *Nanoscale* **5** 6243–8
[9] Zheng G, Mühlenbernd H, Kenney M, Li G, Zentgraf T and Zhang S 2015 *Nat. Nanotechnol.* **10** 308–12
[10] Bozhevolnyi S I 2009 *Plasmonic Nanoguides and Circuits* (Singapore: Pan Stanford Publishing Pvt. Ltd)
[11] Maier S A, Kik P G, Aawater H A, Meltzer S, Harel E, Koel B E and Requicha A A G 2003 *Nat. Mater.* **2** 229–32
[12] Berini P 2007 *J. Appl. Phys.* **102** 033112
[13] Morales A M and Lieber C M 1998 *Science* **279** 208–11
[14] Dionne J A, Sweatlock L A, Atwater H A and Polman A 2006 *Phys. Rev.* B **73** 035407
[15] Foresi J S, Villeneuve P R, Ferrera J, Thoen E R, Steinmeyer G, Fan S, Joannopoulos J D, Kimerling L C, Smith H I and Ippen E P 1997 *Nature* **390** 143–5
[16] Hill M T *et al* 2009 *Opt. Express* **17** 11107–12
[17] Hwang Y, Kim J E and Park H Y 2011 *Opt. Commun.* **284** 4778–81
[18] Han Z, Liu L and Forsberg E 2006 *Opt. Commun.* **259** 690–5
[19] Zeng X, Gao Y, Hu H, Ji D, Gan Q and Bartoli F 2013 *J. Appl. Phys.* **113** 462–93
[20] Zhang M, Fang J W, Zhang F, Chen J Y and Yu H L 2017 *Opt. Commun.* **405** 216–21
[21] Zhu J H, Huang X G and Mei X 2011 *Chin. Phys. Lett.* **28** 054205
[22] Mao J J, Zhai X, Wang L L and Li H J 2017 *Appl. Phys. Express* **10** 082201
[23] Wang T-B, Wen X-W, Yin C-P and Wang H-Z 2009 *Opt. Express* **17** 24096–101
[24] Lin X-S and Huang X-G 2008 *Opt. Lett.* **33** 2874–6
[25] Guo Y, Yan L, Pan W, Luo B, Wen K, Guo Z and Luo X 2013 *Plasmonics* **8** 167–71
[26] Xiao S, Liu L and Qiu M 2006 *Opt. Express* **14** 2932–7
[27] Zhang Z D, Wang H Y and Zhang Z Y 2013 *Plasmonics* **8** 797–801
[28] Setayesh A, Mirnaziry S R and Sadegh Abrishamian M 2011 *J. Opt.* **13** 035004
[29] Tang Y, Zhang Z, Wang R, Hai Z, Xue C, Zhang W and Yan S 2017 *Sensors* **17** 784
[30] Lu F, Wang Z, Li K and Xu A 2013 *IEEE Trans. Nanotechnol.* **12** 1185–90
[31] Lee K S and El-Sayed M A 2006 *J. Phys. Chem.* B **110** 19220–5
[32] Liu N, Weiss T, Mesch M, Langguth L, Eigenthaler U, Hirscher M, Sönnichsen C and Giessen H 2010 *Nano Lett.* **10** 1103–7
[33] Zhang W and Martin O J F 2015 *ACS Photonics* **2** 144–50
[34] Krasavin A V and Zheludev N I 2004 *Appl. Phys. Lett.* **84** 1416–8
[35] MacDonald K F and Zheludev N I 2010 *Laser Photonics Rev.* **4** 562–7
[36] Temnov V V 2012 *Nat. Photon.* **6** 728–36
[37] Chen K, Leong E S P, Rukavina M, Nagao T, Liu Y J and Zheng Y B 2015 *Nanophotonics* **4** 186–97
[38] Wang M S, Zhao C L, Miao X Y, Zhao Y H, Rufo J, Liu Y J, Huang T J and Zheng Y B 2015 *Small* **11** 4423–44
[39] Wang Z and Chumanov G 2003 *Adv. Mater.* **15** 1285–9
[40] Zheng Y B, Yang Y W, Jensen L, Fang L, Juluri B K, Flood A H, Weiss P S, Stoddart J F and Huang T J 2009 *Nano Lett.* **9** 819–25
[41] Si G Y, Zhao Y H, Leong E S P and Liu Y J 2014 *Materials* **7** 1296–317
[42] Khoo I C 2014 *Prog. Quantum Electron.* **38** 77–117
[43] Kossyrev P A, Yin A J, Cloutier S G, Cardimona D A, Huang D H, Alsing P M and Xu J M 2005 *Nano Lett.* **5** 1978–81
[44] Chu K C, Chao C Y, Chen Y F, Wu Y C and Chen C C 2006 *Appl. Phys. Lett.* **89** 103107
[45] Muller J, Sonnichsen C, Poschinger H V, Plessen G V, Klar T A and Feldmann J 2003 *Appl. Phys. Lett.* **81** 171–3
[46] Dickson W, Wurtz G A, Evans P R, Pollard R J and Zayats A V 2008 *Nano Lett.* **8** 281–6
[47] Liu Y J, Hao Q, Smalley J S T, Liou J, Khoo I C and Huang T J 2010 *Appl. Phys. Lett.* **97** 091101
[48] Liu Y J, Leong E S P, Wang B and Teng J H 2011 *Plasmonics* **6** 659–64
[49] Xin H P, Liu F, Ren G J, Zhao H L and Yao J Q 2017 *Opt. Commun.* **389** 92–6
[50] Xie Z-W, Yang J-H, Vashistha V, Lee W and Chen K-P 2017 *Opt. Express* **25** 30764–70
[51] Lee Y, Park M-K, Kim S, Shin J H, Moon C, Hwang J Y, Choi J-C, Park H, Kim H-R and Jang J E 2017 *ACS Photonics* **4** 1954–66
[52] Hsiao V K S, Zheng Y B, Juluri B K and Huang T J 2008 *Adv. Mater.* **20** 3528–32
[53] Liu Y J, Zheng Y B, Liou J, Chiang I-K, Khoo I C and Huang T J 2011 *J. Phys. Chem.* C **115** 7717–22
[54] Liu Y J, Si G Y, Leong E S P, Xiang N, Danner A J and Teng J H 2012 *Adv. Mater.* **24** OP131–5
[55] Si G Y, Leong E S P, Jiang X X, Lv J T, Lin J, Dai H T and Liu Y J 2015 *Phys. Chem. Chem. Phys.* **17** 13223–7
[56] Sullivan D M 2013 *Electromagnetic Simulation Using the FDTD Method* 2nd edn (Piscataway, NJ: IEEE)
[57] Haus H and Huang W P 1991 *Proc. IEEE* **79** 1505–18
[58] Johnson P B and Christy R W 1972 *Phys. Rev.* B **6** 4370–9
[59] Li Q, Wang T, Su Y, Yan M and Qiu M 2010 *Opt. Express* **18** 8367–82
[60] Qiu S L and Li Y P 2009 *J. Opt. Soc. Am.* B **26** 1664–74
[61] Chremmos I 2009 *J. Opt. Soc. Am.* A **26** 2623–33
[62] Ma M, Li S, Jing X and Chen H 2017 *Opt. Eng.* **56** 117109